To link to this article : DOI: 10.1016/j.microrel.2015.12.020
URL : http://dx.doi.org/10.1016/j.microrel.2015.12.020

To cite this version : Bensoussan, Alain *How to quantify and predict long term multiple stress operation: Application to Normally-Off Power GaN transistor technologies*. (2016) Microelectronics Reliability, vol. 58. pp. 103-112. ISSN 0026-2714

How to quantify and predict long term multiple stress operation: Application to Normally-Off Power GaN transistor technologies

A. Bensoussan [1]

Institut de Recherche Technologique Saint Exupery, Department More Electrical Aircraft, Toulouse, France

A B S T R A C T

The present paper is implementing a numerical application of the Boltzmann–Arrhenius–Zhurkov (BAZ) model and relates to the statistic reliability model derived from the Transition State Theory paradigm. It shows how the quantified tool can be applied to determine the associated effective activation energy. The unified multiple stress reliability model for electronic devices is applied to Normally-Off Power GaN transistor technologies to quantify and predict the reliability figures of this electronic type of product when operating under multiple stresses in an embedded system operating under such harsh environment conditions as set for Aerospace, Space, Nuclear, Submarine, Transport or Ground application.

Keywords:
Wide band gap semiconductor
III-nitrides
GaN
GaN-on-Si
Design-for-Reliability
Reliability
Transition State Theory
Quantum statistics
Maxwell–Boltzmann distribution

1. Introduction

The model of the Transition State Theory (TST) developed by E. Wigner [1] and M. Evans and M. Polanyi [2] in 1938 was considered to derive the unified reliability theory presented. Accordingly, the failure rates and reliability mathematics for Cumulative Distribution Function (CDF), Reliability function (R) and Probability Density Function (PDF) have been described when considering the TST concept. In former papers we have demonstrated how multiple stresses applied, may impact the effective activation energy suggested by the BAZ model [3,4]. We will see here how to apply the pre-defined model to the case of a Gallium Nitride Normally-off high power transistor (Enhanced-mode) and a detailed numerical application. The quantified tool will be applied to determine the minimum value of stressor parameters named χ's and the equivalent single associated minimum effective activation energy to predict long term operation under multiple stresses in harsh environment. The completed numerical application on a Normally-off transistor GaN reference GS66508P-E03 650 V enhancement mode manufactured by GaN Systems is proposed to support the methodology. The concepts of maximum rating limits and burnout conditions are key factors which will give insight to derive related stressors as parameters χi's and γ's, both statistically represented by a normal distribution law.

The paper is organized as follows: after a recall of the principle of the generalized BAZ model, we will take the example of a Normally-Off GaN Power transistor detailing from the data sheet the maximum rating limits and will show other dynamic maximum rating limits to be considered in detail mainly related to the switching bias operation conditions (also related to design rules). Finally the BAZ model will be refined and adapted to this technology. A short discussion will recall the main highlights we have observed.

2. BAZ model and Transition State Theory

Shown in Fig. 1, is a free energy diagram of why things generally tend to degrade faster at higher temperatures as explained in chemistry and Reliability Physics books (see for example J.W. McPherson [5]). Stress-dependent activation energy observations seem to be general in nature (i.e., not confined just to a single failure mechanism or stress type), and works attempt to explore the conditions under which a stress dependent activation energy is theoretically expected. The generalized Eyring model presented by McPherson has been refined under the BAZ model [3,4].

Fig. 1 is simply related to the general model called Boltzmann–Arrhenius–Zhurkov (BAZ) also described by the Transition State Theory (TST) [1,2]. We have seen the stress factor γ. *S* can precisely counterbalance the Arrhenius activation energy E_a for a device at burnout due to an overstress (i.e. the energy of the transition state with burnout catalyst effect is at the same level as the initial state energy). In this case this

E-mail address: alain.bensoussan@irt-saintexupery.com.

[1] Permanent address: Thales Alenia Space France, Competence Center Electronics (CCEL), Toulouse, France.

http://dx.doi.org/10.1016/j.microrel.2015.12.020

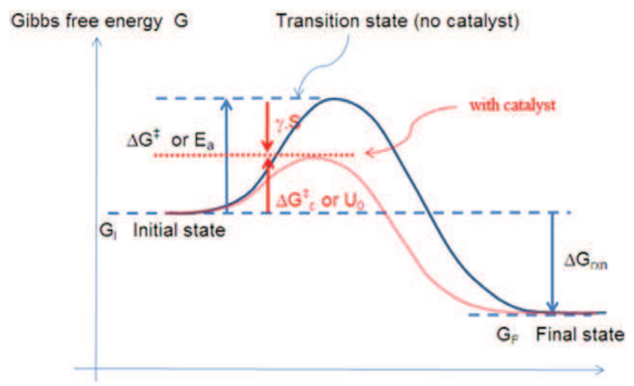

Fig. 1. Suggested TST applied to reliability (from Ref. [1]).

works for any failure mechanism that is thermally determined as a rate function described by the Maxwell–Boltzmann distribution.

We have expressed the BAZ model as the lifetime τ defined by the following equation:

$$\tau = \tau_0 \cdot \exp\left[\frac{E_a}{k \cdot T_{eff}} \cdot c(\chi_i \cdot \gamma_i)\right] \tag{1}$$

With a dimensionless energy factor parameter $c(\chi_i \cdot \gamma_i)$ given by:

$$c(\chi_i \cdot \gamma_i) = 1 - \frac{k \cdot T_{eff}}{E_A} \cdot \sum_{i=1}^{M} (\chi_i \cdot \gamma_i \cdot S_{iBO}) \tag{2}$$

where the S_{iBO} is the corresponding maximum catastrophic burnout failure limit related to each electrical stress parameter for $i = 1$ to M (current, voltage and power), T_{eff} is the absolute temperature that could depend also on the applied stress χ_i when the Joule effect is occurring, τ_0 is the time constant, and γ_i is the factor of loading characterizing the weight of the level of stress. This equation is seen as the generalization of the Eyring model as demonstrated in [2]. Indeed, when the stress parameter is set to S_{iBO} leading to a sudden catastrophic failure we have:

$\chi_i = 1$ and $c(1) = 0$ allowing calculating γ_i for a combination of stress parameters as:

$$E_a = k \cdot T_{eff} \cdot \sum_{i=1}^{M} (\gamma_i \cdot S_{iBO}). \tag{3}$$

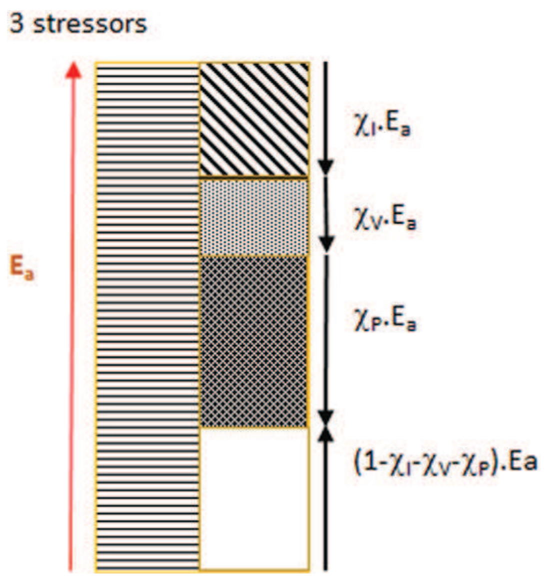

Fig. 2. Schematic of equivalent effective activation energy w.r.t. three stressor contributions.

Because every χ_i is in the range [0; 1], this equation shows that the activation energy is compensated by a linear combination of stressor energies associated with each parameter.

When considering the simplest configuration where the main stressor is the breakdown voltage characterized by a term χ_V, suppose other stressors χ_j to be equal to 0. Eq. (4) for $\chi_V = 1$ will allow determining γ_V as:

$$\gamma_V = \frac{E_a}{k \cdot T_{eff} \cdot V_{BO}} \tag{4}$$

Combining Eqs. (4) and (2) leads to:

$$c(\chi_V \cdot \gamma_V) = 1 - \chi_V. \tag{5.a}$$

We have seen similar equations can be obtained for other stressors when considered alone:

for pulse power dissipation[2]

$$c(\chi_P \cdot \gamma_P) = 1 - \chi_P \tag{5.b}$$

for current

$$c(\chi_I \cdot \gamma_I) = 1 - \chi_I. \tag{5.c}$$

Because the principle of superposition is not valid, it is understood that the situation is different when considering a multiple stressor configuration applied simultaneously.

Considering the situation of three stressors: a) χ_I related to current limited by the maximum allowed current characterized by I_{BO}, b) the breakdown voltage characterized by a term χ_V and V_{BO}, and c) stressor χ_P related to power consumption related to the maximum allowed dissipation characterized by P_{BO}.

Saying Eqs. (5.a), (5.b) and (5.c) are constrained by the boundary conditions defined for the burnout limits (subscribe BO), we obtained:

$$c(\chi_i \cdot \gamma_i) = 1 - \frac{k \cdot T_{eff}}{E_a} \cdot [(\gamma_I \cdot \chi_I \cdot I_{BO} + \gamma_V \cdot \chi_V \cdot V_{BO} + \gamma_P \cdot \chi_P \cdot P_{BO})]. \tag{6}$$

Merging Eq. (6) with Eq. (4), we were able to normalize burnout parameters and we got an expression of coefficient $c(\chi_i;\gamma_i)$:

$$c(\chi_i \cdot \gamma_i) = c(\chi_I;\chi_V;\chi_P) = 1 - \chi_I - \chi_V - \chi_P. \tag{7}$$

The simple schematic drawing given in Fig. 2 details contributions of stressors when three stressors are simultaneously applied as per Eq. (7).

The next chapter will show how a numerical application on a Power GaN Normally-Off transistor enhancement mode GaN transistor is implemented.

3. A Normally-off transistor GaN: data sheet and maximum rating definitions

As an example, the data sheet given (at the date of this publication) in Table 1 defines the parameters extracted from a Power GaN Normally-Off transistor GS66508P-E03 650 V enhancement mode GaN transistor (reproduced from data sheet GaN Systems www.gansystems.com).

Generally, maximum rating limits are defined and are considered with a given margin compared to burnout failure limits (M_I, M_V or M_P respectively for current, voltage and power dissipation).

Sudden catastrophic failures due to electrical overstresses can be characterized for each transistor lot. This consideration will help to define the *sine qua non* condition to consolidate the reliability model.

[2] Pulse power dissipation or commutation losses needs (turn-on and turn-off energies) to be considered when using such Normally-off transistors in their application because of the switching time conditions from off-state to on-state operation can stress the device close to the limit of its SOA in pulsed mode.

Table 1
Example of preliminary data sheet of GS66508P-E03 650 V enhancement mode GaN transistor. Reproduced from GaN Systems www.gansystems.com.

Symbol	Parameters	Value	Units
Absolute maximum ratings (at Tcase = 25 °C unless otherwise noted)			
T_J	Operating junction temp.	−55 to +150	°C
T_S	Storage temperature range	−55 to +150	°C
$V_{DSmax\text{-}rating}$	Drain-to-source	650	V
V_{GS}	Gate-to-source	±10	V
$I_{DS(cont)25}$ (or $I_{DS\text{-}MR}$)	Continuous drain current (Tcase = 25 °C)	34	A
$I_{DS(cont)100}$	Continuous drain current (Tcase = 100 °C)	20	
$I_{D,pulse}$ (or $I_{D\text{-}pulse\text{-}MR}$)	Pulsed drain current (Tcase = 25 °C) (note 1)	45	A
Note 1: Limited by saturation			
Thermal characteristics (typical values unless otherwise noted)			
$R_{\theta JC}$	Thermal resistance (junction to case)	0.5	°C/W
$R_{\theta JA}$	Thermal resistance (junction to ambient)	55	°C/W
Device mounted on PCB (see corresponding datasheet for detail)			

Electrical characteristics (at Tcase = 25 °C unless otherwise noted)

Symbol	Parameters	Typ. value	Units	Conditions
BV_{DSS}	Drain-to-source breakdown voltage	650	V	VGS = 0 V, I_D = 3.3 μA/mm
$R_{DS(ON)}$	Drain-to-source on resistance	52	mΩ	V_{DS} = 7 V, T_J = 25 °C, I_D = 9 A
$V_{GS(th)}$	Gate threshold voltage	1.6	V	$V_{DS} = V_{GS}$,
I_D = 7 mA				
I_{DSS}	Drain to source leakage current	2	μA	V_{DS} = 650 V
V_{GS} = 0 V, T_J = 25 °C				
I_{GSL}	Gate to source leakage	200	μA	V_{GS} = 7 V,
V_{DS} = 0 V				
V_{plat}	Gate plateau voltage	3	V	V_{DS} = 400 V
V_{SD}	Source–drain reverse voltage	3.0	V	V_{GS} = 0 V, T_J = 25 °C, I_{SD} = 9 A

Multiple stresses can be seen as a juxtaposition of stress amplitudes (not the superposition principle) leading to reduce proportionally the effective activation energy up to a zero value maximum limit (in this case the activation energy is exactly compensated by the cumulated stress factors). Let's consider the following notation for burnout conditions (also supposed to be described by a normal distribution) (see Fig. 3 for labeling conditions compared to the Safe Operating Area (SOA)):

Off-state drain current $V_{DSoff\text{-}BO}$ (condition 3)

- On-state drain current at saturation $I_{DSon\text{-}BO}$ (conditions 1, 2 & 4),
- Maximum power dissipation during on-off nominal operation $P_{DS\text{-}DC\text{-}BO}$ (conditions 5 and 6 to 8).

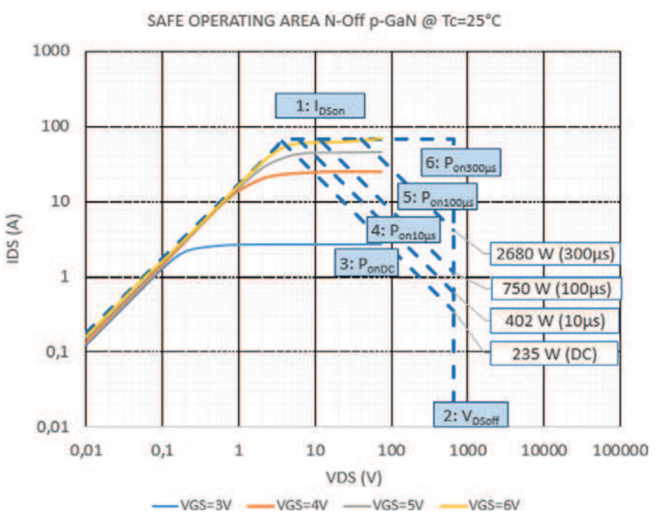

Fig. 3. Safe operating area of Normally-Off GaN transistor showing boundary conditions defined for χ and γ parameter determination.

When conducting evaluation and qualification testing sequences as depicted in MIL Standards or similar, such DC stress tests are foreseen. We propose to implement such qualification test sequence and biasing depicted in Fig. 3 in the frame of the Robustness project we are conducting. The results will be presented in another paper in a future study. But indeed, they have several drawbacks:

a) They are focused on validating simple stress conditions including high temperature stress superposed with a single DC bias stress at a time,
b) They are based on the Arrhenius law considering accelerating factors managed by high temperature effects forgetting low temperature effects,
c) They generally don't address dynamic stress conditions (even RF or switching in operation) at high or low temperature.

SOA limits are defined for DC stresses but are half-finished when considering nominal operating conditions. They must be completed by switching stress conditions to be imposed to the designers. In order to highlight how the design rules must be taken into account, the next paragraph will provide such major inputs.

4. A Normally-off transistor GaN: reliability impact of turn-on/turn-off switching voltage induced by commutation losses

Since Normally-off GaN transistors start to conduct significant current at $V_{GS}(th)$ = 1.6 V, care must be taken to ensure a low impedance path from gate to source when the device needs to be held off during dv/dt in a rectifier function. As the temperature coefficient of the eGaN FET is positive throughout its range of operation, this means that when the temperature of a localized region of the device increases, its current carrying capability is reduced causing the current to be dispersed to other areas of the die. This dispersion of the current equalizes the temperature of the die, and is known as "self-ballasting." The power MOSFET, on the other hand, has a significant region of negative temperature coefficient operation (below 5.0 V on the gate) where there is no self-ballasting.

Operation within this region creates localized hot spots within the die and, thus, limits the SOA capability of the die.

These considerations have been explained on literature by B. Cogo et al. [6,7] and J. Brandelero et al. [8]. From these papers, power device modeling published articles have shown turn-on turn-off switching voltage characteristics induced by commutation losses. Losses in the switches are usually the most important point to be considered in a converter design; however, switching losses are not always provided in datasheets. The following text is mainly inspired from large extract from the three papers.

As implemented in [7], turn-on and turn-off energies could be accurately determined separately for different switched voltages and currents by controlling the commutation of a full bridge in two different modes. The authors argue that due to the packaging of GaN EPC© devices, current measurement into device is not possible with a Rogowski probe or a current transformer without changing the power loop. This is also the case for almost all low voltage Silicon MOSFET packaging. Since the opposition method is a non-invasive method, it is suitable to be used to measure switching losses of “wide bandgap” devices. The opposition method consists of an association of two identical converters supplied by the same source, one operating as a generator, the other as a receptor (as shown in Fig. 4). Thus, a test bench using the opposition method was implemented in [8] to characterize switching energies, under actual working conditions, of an EPC1001 GaN power transistor. Consideration of such commutation (ripple) induced stresses is presented in Fig. 5, showing an overview of switching losses in a buck converter operating in two different modes: low current and high current ripple modes.

The authors have considered other losses as listed below:

- Inductor losses,
- Transistor conduction losses,
- Connection losses,
- Bus capacitor losses.

Taking into account such parasitic effects, we propose to introduce three (3) new stress factors at burnout failure limits which can be responsible for impact and degrade effective activation energy, including:

- *Turn-off controlled commutation*
  - o Energy turn-off dynamic switching $E_{off\text{-}surge}$ (energy factor $\chi_{Eoff\text{-}surge}$),

- *Turn-on controlled commutation*
  - o Transistor turn-on energy E_{on_surge}, which includes the reverse recovery losses of the body diode (energy factor χ_{Eon_surge})
  - o Turn-on dynamic switching for $V_{GS\text{-}surge}$ (energy factor χ_{VGSon_surge}).

Recalling chapter II and these parasitic effects, we can express the energy factors as a juxtaposition of stressor parameters as listed in Table 2 each of them defined by their γ parameters and their associated χ's bounded by their maximum rating limits calculated from Eqs. (4) and (5.a), (5.b) and (5.c). To do so, activation energy related to the

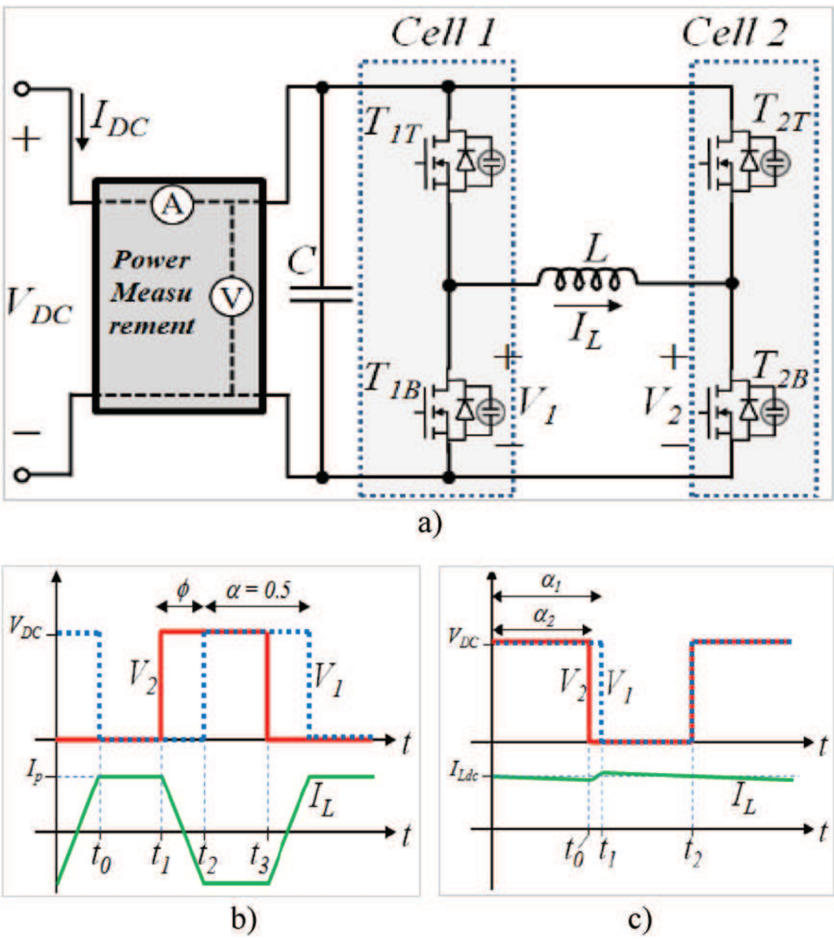

Fig. 4. a) Circuit used in the proposed method to measure switching energy of transistors, b) typical voltage and current waveforms for the “turn-off loss measurement mode” and c) for the “turn-on loss measurement mode”.
From [7].

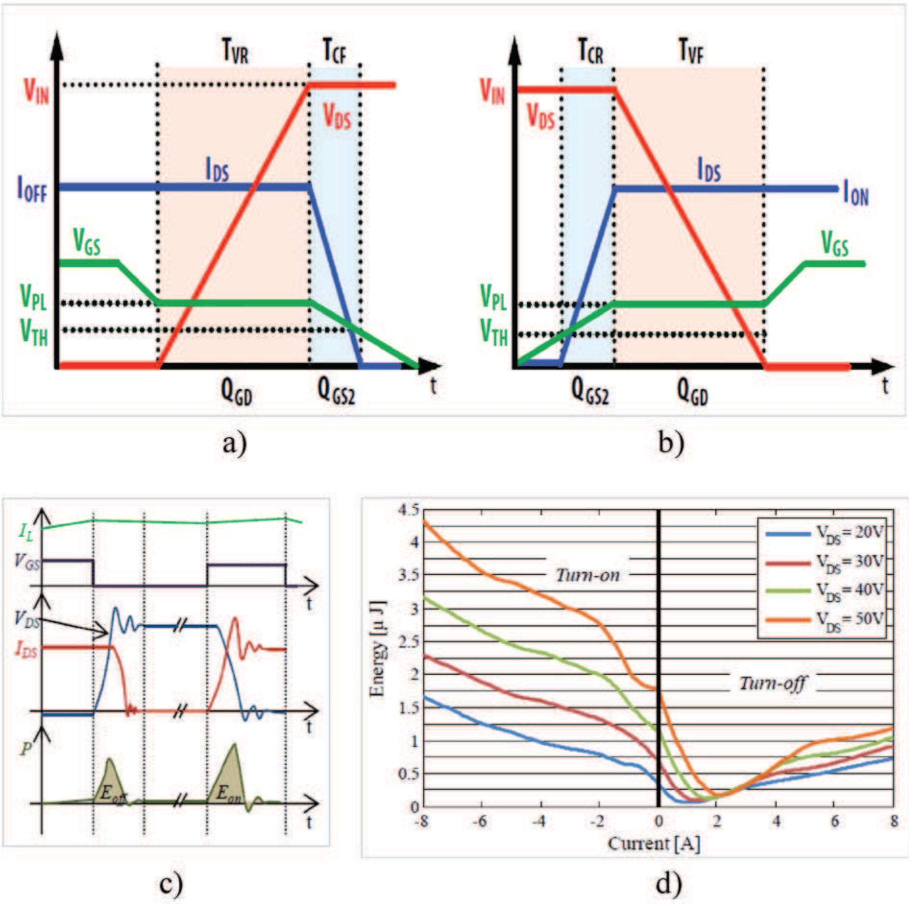

Fig. 5. Ideal Hard Switching (extracted from EPC WP009) for a) turn-off transition, b) turn-on transition, c) typical turn-off energy calculation (from [8]) based on switch voltage and current and d) measured switching energy for different switched currents and voltages, for the 100-V eGaN FET EPC1001.

ohmic contact (TiAl:GaN system based alloy) and Schottky contact (TiN:GaN system alloys) are considered for EPC technology.

As summarized by Del Alamo in 2009 [9], relatively high activation energies have been reported from 1.05 to 2 eV for GaN technologies. This paper highlighted *an electrical degradation mechanism for GaN HEMTs that is associated with the strong piezoelectric nature of GaN and AlGaN. Under high voltage conditions, the high electric field that is produced introduces strong tensile stress in the AlGaN barrier layer that peaks right below the gate edge. This results in an increase in stored elastic energy inside the AlGaN. If exceeding a critical value, crystallographic defects are formed that are electrically active. The damage consists of dimples, cracks crystallographic damage on the drain side of the device right next to the gate edge. These have shown the presence of prominent that extent through the AlGaN but stop at the GaN interface and, in extreme cases, metal diffusion from the gate down the crack. In addition, the level of crystallographic damage correlates with the degradation in the electrical characteristics of the device.*

Linking to Eq. (3), and as a preliminary analysis, let's consider the activation energy associated with metallurgical diffusion mechanism as the main effect characterized by a value close to 2.1 eV. Of course this value must be assessed and confirmed on a given GaN technology process after a series of simple high temperature storage test sequences. The effective junction temperature T_{eff} must also be related to the case temperature and the thermal resistance of the junction case.

Table 2
List of the 10 stressor parameters and related values used impinging on the effective activation energy applied to GS66508P-E03 650 V enhancement mode GaN transistor (assuming E_a and T_{eff} — see detail in text).

		Parameter	Maximum rating values (MR)	DC limit BO	DC BO values	Dynamic biasing stressors	Surge BO limits	Transient stressors	Transient BO limits	γ (Eq. 4)	Calculated γ values at $T_{eff} = 298$ K	$\chi_{i\ MR}$
1	Current	I_{DSon}	34 A	I_{DSonBO}	68 A					γ_{IDSon}	1.20	50%
2		I_{DSon_dyn} (@ 10 μs)	45 A					I_{DSon_sgeBO}	90 A	γ_{IDSsge}	0.91	50%
3	Voltage	V_{DSoff}	650 V	$V_{DSoffBO}$	900 V					γ_{VDSoff}	0.091	50%
4		V_{GSon} (@ I_{DSonMR})	10 V					V_{GSon_sgeBO} (@ 10 μs)	20 V	γ_{VGSon}	4.09	50%
5	Power	P_{DSonDC}	235 W	P_{DSonBO}	470 W					γ_{PDSon}	0.17	50%
6.1		P_{onDYN}	402	@ 300 μs		$P_{on300BO}$	574 W			$\gamma_{PonDYN300}$	0.14	70%
6.2			750 W	@ 100 μs		$P_{on100BO}$	1072 W			$\gamma_{PonDYN100}$	0.076	70%
6.3			2680 W	@ 10 μs		P_{on10BO}	3830 W			$\gamma_{PonDYN10}$	0.021	70%
7	Energy	E_{offDYN}	7 μJ					E_{off_sgeBO}	20 μJ	γ_{Eoff_sge}	4.09	35%
8		E_{onDYN}	7 μJ					E_{on_sgeBO}	20 μJ	γ_{Eon_sge}	4.09	35%

Calculated values for γ at $T_{eff} = 298$ K (Eq. (3)) and χ_{iMR} (Eq. (4)) are completed in Table 2 (assuming the Boltzmann constant $k = 8.61733 \cdot 10^{-5}$ eV·K^{-1}) and $E_a = 2.1$ eV. These parameters are related to burnout parameter limits from which we know they are characterized by a Gaussian or Standard distribution law. Consequently each of them can be written in terms of mean and standard deviation factor as follows:

$$f_{sd}\left(S_{iBO_{failure}}\right) = \frac{1}{\sigma_{iBO} \cdot \sqrt{2\pi}} \cdot e^{-\frac{1}{2}\left(\frac{S_{iBO_{failure}} - \overline{S_{iBO}}}{\sigma_{iBO}}\right)^2} \quad (8)$$

where $\overline{S_{iBO}}$ and σ_{iBO} are respectively the mean and the standard deviation of statistical distribution law of every $S_{iBO_{failure}}$.

5. BAZ model applied to Normally-off GaN transistor

As a result the related parameters χ_i's are statistically represented by a similar distribution law and Fig. 7 represents a 3D-plot of such normalized stress factor χ_i vs the catastrophic burnout limit $Si_{BO\_failure}$ of a Normally-off transistor GaN. When a parameter failure limit is affected by the temperature as for example observed on breakdown voltage decreasing when the temperature is decreasing [10], this effect can be easily considered within the reliability model thanks to the γ_V parameter.

In this example we have considered normalized stress conditions and we can see the behavior of the coefficient $c(\chi_I, \chi_V, \chi_P)$ for three χ_P values (from 0 to 0.5) and varying χ_I and χ_V from 0 to 1. Having such a mapping, we need to consider that the χ_i parameters are limited by their maximum rating values as given in Table 3 and thus the value achievable by the coefficient $c(\chi_I, \chi_V, \chi_P)$ is quantified when multiple stresses are combined. Accordingly the related triplet (χ_I, χ_V, χ_P) can be calculated and a new reliability criterion can be drawn which relates simply as a single condition all constraints associated with E_a, all derating limits (both statics and dynamics) and thermal condition. We propose to set coefficient $c(\chi_I, \chi_V, \chi_P)$ verifying:

$$c\left(\chi_I, \chi_{V,} \chi_P\right) > 30\%. \quad (9)$$

This value is chosen in order to guarantee an effective activation energy greater or equal to 0.7 eV for a worst case wearout failure mechanism. In such a case, to demonstrate long term life in operation for Space Application as shown in Fig. 6, we will need to run sampling devices under biasing for a 3000 hour endurance lifetest sequence at $T_{eff} = 280$ °C (to achieve 80% lot failure) in order to be equivalent to 30 years at $T_{eff} = 110$ °C (for 0.1% failure). Note that this is equivalent to MTTF (@110 °C) = 1.5 million hours or more than 170 years.

Now, we can draw the major conclusion of this section that is: when multiple stresses are applied simultaneously, the derating parameters and their maximum rating limits values need to be set in order to counterbalance an equivalent activation energy not inferior to 30% of E_a. Iso-planes $c(\chi_I, \chi_V, \chi_P) =$ constant, are shown in Fig. 7 and represent combination of triplet rates to get a given value of $c(\chi_I, \chi_V, \chi_P)$ in view to satisfy a foreseen activation energy goal.

The drawing in Fig. 8 presents the methodology to determine operating worst case conditions which can be supported by the device

Table 3
Electrical parameter limits for voltage and power stressors.

Parameter limits	V_{DSoff}	P_{DSoff}
@ Burnout (a)	900 V	470 W
@ Maximum rating (b)	650 V	235 W
@ Derating limits (c)	487.5 V	117.5 W
X_{ioff} (c)/(a)	54.2%	25%

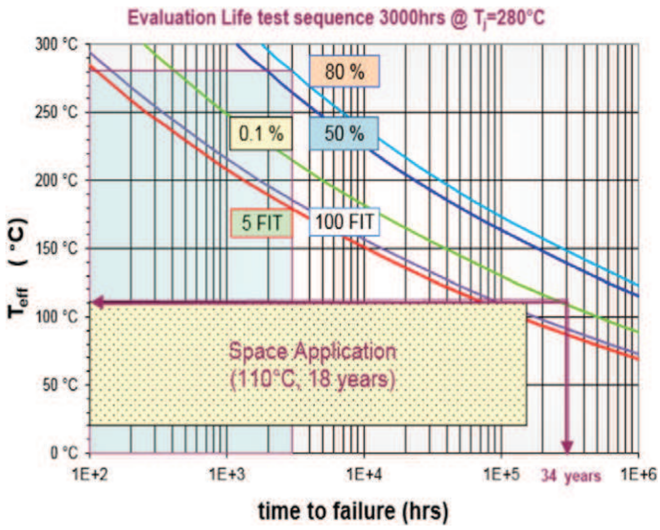

Fig. 6. Probability of failure vs T_{eff} and time t (assuming $E_{aeff} = 0.7$ eV). The lifetest sequence proposed on top will demonstrate less than 0.1% failure at 110 °C after 34 years).

under operating conditions and environmental multiple stressors in order to guarantee a time to failure rate of less than 1% after 30 years at junction temperature lower or equal to 110 °C as shown Fig. 6.

In the same spirit we defined the stressor energy concept (γ linearly proportional) and we can introduce a new concept for the internal energy of a device to be a straightforward linear relation with the electrical mode under consideration. Gradual degradation or sudden catastrophic ones are evidenced and signed by electrical failure modes. In the following we will try to define the mathematics of this perception.

6. A numerical application example for a Normally-off GaN transistor

In the following we are assessing the multi-stress induced effect the reliability figures on a GS66508P-E03 650 V enhancement mode Normally-off GaN transistor. The Arrhenius activation energy due to thermal stress only is assumed to be $E_a = 2,1$ eV.

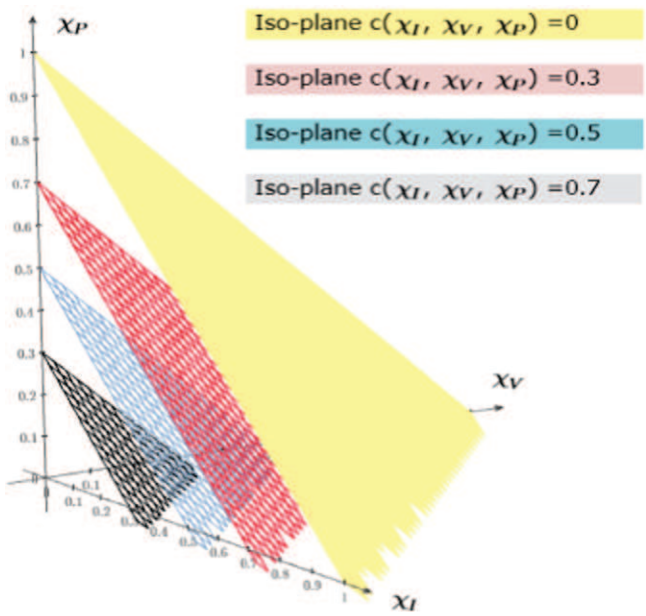

Fig. 7. 3D-plot of normalized stress factor χ_i.

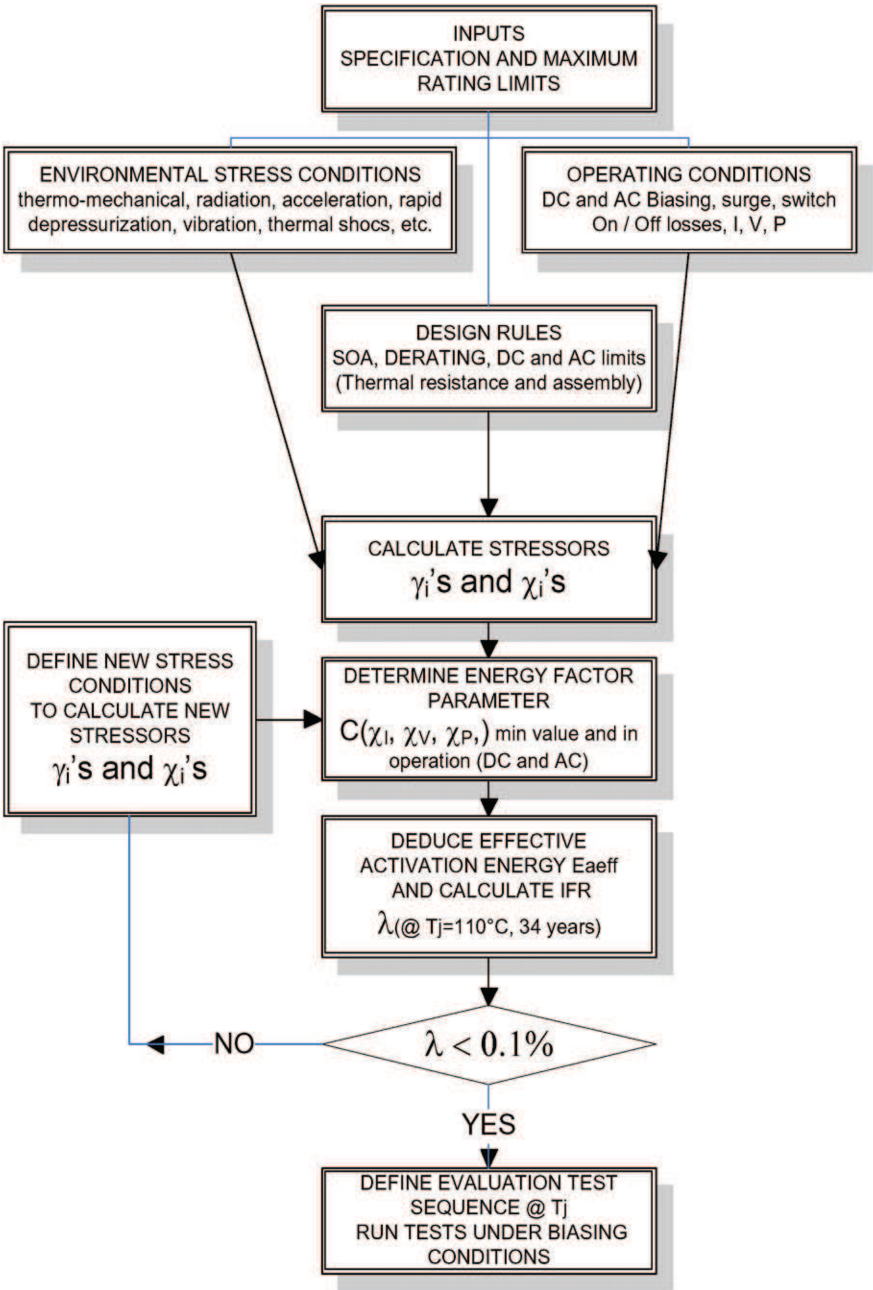

Fig. 8. Methodology for determination of evaluation test sequence for a 0.1% failure rate after 34 years at junction temperature lower or equal to 110 °C.

In order to assess the reliability model and to define the limits of the Safe Operating Area (SOA) we need to define some specific condition of endurance testing with high enough stress to accelerate failure mechanisms.

Future reliability test programs are designed in order to simulate and accelerate various failure mechanisms one at a time. Power converter equipment based on Normally-Off GaN transistors as shown in Section 4 are designed in order to minimize to a less extent the commutation losses. Switching conditions between off and on states with short transition time are implemented but such losses cumulated during operation may generate multiple stress behavior. In order to simulate such operation we can design a reliability test program with two kinds of stress test at high V_{DSoff}. The BAZ model proposed helps to simulate such occurrence of multiple stress conditions and to take into account their interactions.

Let's consider two types of stresses imposed simultaneously:

a. the off-state at VDS close to the breakdown voltage or close to burn-out of the transistor: i.e. the Voltage stressor
b. the I_{DS} current at high VDS induced during the switching time which can be set under equivalent static condition to simulate the Joule effect induced by commutation losses: i.e. the Power stressor.

The following will explain how to handle these stresses in parallel and to assess the combined activation energy to be considered for accelerating factor determination.

Space industry defines maximum rating and associated derating condition for safe operation in use as the following: voltage should never exceed 75% of the maximum rating of any voltage (V_{DS} or V_{GS})

and currents (I_{DS}) and never exceed power dissipation greater than 50% of the maximum rated power dissipation. In addition to that $T_{junction}$ must remain lower than 110 °C during the flight mission.

As per data measurements performed of COTS samples on the GaN transistor GS66508P-E03 650 V we obtained the following Table 3:

Eq. (7) factor $c(\chi_i; \gamma_i)$, gives the value of this term when mechanisms Voltage Stressor and Power Stressor are applied:

$c(\chi_i; \gamma_i) = 1 - 54.2\% - 25\% = 20.8\%$..

When the two stressors are applied simultaneously at their derating limits, the effective activation energy is reduced to 0.437 eV. Such activation energy is reducing drastically MTTF foreseen for Space application and then even compliant to Space rules the MTTF is no more acceptable.

When stressor percentages are lowered by reducing V_{DS} voltage to 330 V and Pdiss to 140 W their contribution to the effective activation energy is 33.6% of E_a (i.e. 0.7 eV) as shown in Fig. 7. In other words this model helps to assess the impact of the mission profile on the final activation energy expected and then assesses margin to Design for Reliability Space equipments. We need to be very careful when applying Quality Standards which are not considering multiple-stressor impacts and new rules for HiRel application are recommended to be set accordingly.

7. The BATHTUB curve model

Considering N "good" devices of interest randomly selected from a homogeneous manufacturing lot. The term "good" means the devices are non-discernible, they are functional and their performance and electrical parameters are statistically normally distributed (Gauss or Normal statistics). Let's consider the most representative electrical parameters (biasing or leakage currents, biasing or breakdown voltages) to be a representative sensor of the healthiness of the devices. For the sake of simplicity, we focus on the failure mode used for reliability consideration which is the most representative electrical parameter. Such a parameter can be considered as a signature or saying a measure of the internal energy ϵ as referred in Fig. 9 where for example be the pinch-off drift of a GaAs MESFET technology plotted as a square root of time degradation mechanism (gate sinking metal diffusion in active layer). This Fig. 9 is a schematic drawing of the TST and applied to the reliability of

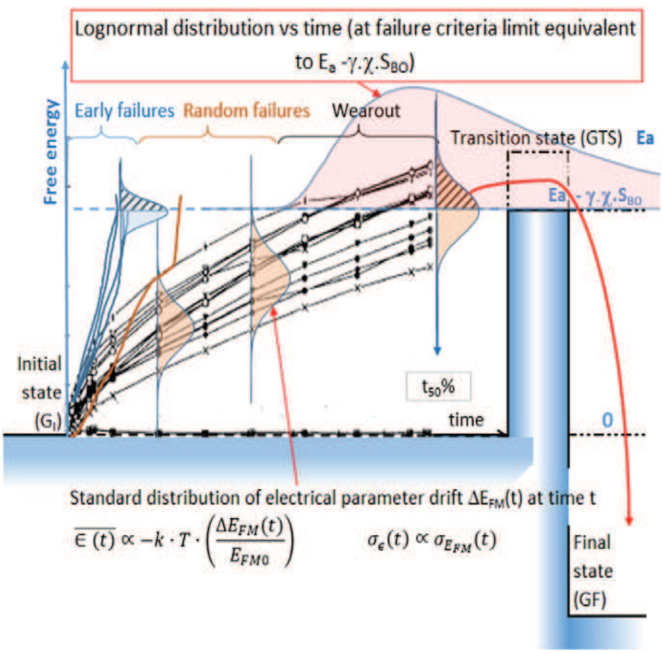

Fig. 9. Effect of failure phases (Early, Random and Wearout) deduced from Transition State Theory.

electronic parts showing how the BAZ model is applying. Other mechanisms as Early Failure or Infant Mortality and Random Failures are positioned as they may occur earlier assuming different gradients of degradation time (assumed to be linear or super linear).

7.1. How to determine the distribution function or the probability for a device at energy state ϵ.

Because devices are characterized by their electrical parameters measured experimentally we have a physical indicator tool to quantify the energy change during aging and saying the drift of a parameter failure mode $\Delta E_{FM}/E_{FM0}$ is directly linked to the internal energy as:

$$\overline{\varepsilon(t)} = -\alpha_1 \cdot kT \left(\frac{\overline{\Delta E_{FM}(t)}}{E_{FM0}}\right) \tag{10.a}$$

$$\sigma_\varepsilon(t) = \alpha_2 \cdot \sigma_{E_{FM}}(t) \tag{10.b}$$

where E_{FM0} is the electrical parameter measured at t = 0. $\Delta E_{FM}(t)$ and $\sigma(t)$ are respectively the mean and the standard deviation of electrical parameter (Gaussian distribution) depending on aging time.

Eqs. (10.a) and (10.b) are supported by the fact that Free energy of a device is proportionally increasing with temperature; when the failure mode degrades. Consequently, the Free energy increases with time (the sign "−" is introduced because percentage of parameter drift is negative).

Thus, the probability density function is now assumed to be a function of the energy at time t described by a Gaussian distribution law:

$$f(\varepsilon, t) = \frac{1}{\sigma_\varepsilon(t) \cdot \sqrt{2\pi}} e^{-\frac{1}{2}\left(\frac{\varepsilon - \overline{\varepsilon(t)}}{\sigma_\varepsilon(t)}\right)^2}. \tag{11}$$

Knowing this probability density function and recalling the set of equations we are able to model:

A) Wearout failures based on:

- The number of failed device at time t assumed to be Wearout failure:

$$N_{Fail}(t) = \int_{U_0 - \gamma \cdot S}^{\infty} \rho_{wearout}(\varepsilon) \cdot f_{wearout}(\varepsilon, t) \cdot d\varepsilon. \tag{12}$$

- The number "Good" devices defined by:

$$N_{Good}(t) = \int_0^{U_0 - \gamma \cdot S} \rho_{wearout}(\varepsilon) \cdot f_{wearout}(\varepsilon, t) \cdot d\varepsilon. \tag{13}$$

- The normalization when considering the total number of device is given by:

$$N_T(t) = N_{Good}(t) + N_{Fail}(t) = \int_0^{\infty} \rho_{wearout}(\varepsilon) \cdot f_{wearout}(\varepsilon, t) \cdot d\varepsilon. \tag{14}$$

B) Random failures:

- Random failure mechanisms can be discriminated versus time in Eqs. (12) to (14) considering that the appropriate distribution function or probability that a device at energy state E is defined by a function of energy $f_{random}(E)$ and assuming the adequate density of states, or the number of energy states per unit volume in the interval ΔE is $\rho_{random}(E)$.

C) Infant mortality model

- Infant mortality is defined by Eqs (12) to (14) considering that the appropriate distribution function or probability that a device at energy state E is defined by a function of energy $f_{infant}(E)$ and the adequate density of state or the number of energy states per unit volume in the interval ΔE is $\rho_{infant}(E)$.

Early failure, random failure and wearout mechanisms can be discriminated with time thanks to Eqs. (12), (13) and (14) respectively accommodated in order to depict the full bathtub curve. Doing so, the Instantaneous Failure Rate (IFR) $\lambda(t)$ is defined by:

$$\lambda(t) = \frac{N_F(t)}{N_T(t)} = \frac{\int_{U_0-\gamma \cdot S}^{\infty} \rho(\varepsilon, t) \cdot f(\varepsilon, t) \cdot d}{\int_{0}^{\infty} \rho(\varepsilon, t) \cdot f(\varepsilon, t) \cdot d} \tag{15}$$

with the corresponding superposition of failure mechanisms and their appropriate definitions.

All these equations are linked to the suitable densities of state $\rho_{infant}(E)$, $\rho_{random}(E)$ and $\rho_{wearout}(E)$. Appendix A is describing how such densities of state can be calculated and quantified based on a Maxwell–Boltzmann statistical approach.

8. Discussion

The generalized BAZ model based on simultaneous multiple stress conditions has been presented and is fully depicted thanks to considering absolute maximum ratings and burnout limit normalization. The methodology implemented for the GaN transistor process in Section 5 can be easily generalized to any type of electronic device for any failure mechanism that is thermally determined as a rate function described by the Maxwell–Boltzmann distribution.

To complete our study, here are some views related to advantages and comments of the proposed methodology.

To illustrate this, let's considering Hot Carrier Injection mechanism and impact ionization stress mechanism. They are mostly observed to have higher failure rates at low temperature than at high temperature. Hence, negative activation energy must be set for low temperature range while positive activation energy must be introduced for high temperature range.

The BAZ model is a single effective activation energy representing no more than one effective mechanism. For multiple activation energies, we have to consider that the multiple mechanisms are statistically independent and they must be dealt with a stochastic process. This will allow the total equivalent failure rate at any temperature and/or combination of stresses to be a sum of FIT. This is exactly what the approach proposed by J. B. Bernstein [11,12] is offering as related to the Multiple High-Temperature Operating Life (M-HTOL) test. It can certainly be an outstanding combination with the BAZ model. This merging will be studied and developed in a future paper in preparation with J.B. Bernstein.

8.1. Advantages

The Transition State Theory was set in the generalized BAZ model. It helps to elaborate a useful tool aiming to develop a methodology to define, quantify and predict the complete reliability Bathtub curve for any electronic device. Furthermore, it takes into consideration a combination of multiple stress conditions merging intrinsic and extrinsic constraints and electrical modes. It provides a good simple support to model the catalyst effect induced by many stressors as for example thermal and dynamic biasing or radiation stresses. Anticipating combined effects due to various stressors, we have shown how efficient is the model applied to new emerging technologies as GaN processes: helping to quantify and reduce evaluation and qualification test time sequences. There is no need to conduct multiple stress test sequences rather it is proposed to perform only a simple storage stress associated to deep electrical characterization and develop a good knowledge of physics of failure (based on very detailed constructional analyses and failure analysis methods).

The generalized BAZ model takes into consideration other stressors than temperature defining accelerating factor for DC and AC parameters in a simultaneous combined form. It is applicable to support low temperature acceleration models as well.

Finally, the model is easy to be implemented and consolidated and provides a useful tool for determining and recommending design rule consideration for breakthrough technologies: it covers Design for Reliability methodologies as required in the Prognostics and Health Monitoring (PH&M) paradigm.

The generalized BAZ model is an extension of the Arrhenius law not only applicable to diffusion and storage test stresses but also valid for other combined harsh environment stressors cumulated with temperature.

8.2. Other comments

Of course the generalized BAZ model is supported by the hypothesis that the internal energy of a device is perceived or observed by an electrical mode signature: either a leakage current of a performance parameter. This is not always the case as some hidden failure mechanisms can be activated (i.e. not seen as continuous electrical degradation but rather as sudden catastrophic failure). This is noticed for latent (cumulated or not) effects (due to contaminants, ESD, EOS, increase of dislocation density, radiation as displacement damage DD for example) or even for crystal dislocation accumulation in active and non-active regions. When these physical and/or electrical precursors are not yet active, they can be later activated by temperature and electrical stressors.

In all these particular cases, the generalized BAZ model is failing or less accurate to predict failure and the end of life limit. If so, the Early Failure or the Random Failure stages of the Bathtub curve can be overestimated. On the one hand, one needs to identify failure analysis techniques or electrical characterization method to pinpoint electrical precursors to model the behavior of the reliability. On the other hand, it is necessary to collect and validate how the stressors are acting to accelerate the failure mechanisms expected.

These limitations of the generalized BAZ model will require some refinement or new techniques of characterization to be instigated. We will address such considerations in our future studies and in particular for the case of small size node (lower than 30 nm) of Si semiconductor integrated processes called Deep-Sub-Micron (DSM) technologies.

8.3. Special care to be considered when applying this methodology — how to consolidate it?

Existing and new failure analysis techniques need to be controlled and implemented. Similarly, constructional analysis and knowledge of semiconductor physics modeling are pre-requisites in any case. These two prerequisites will let us understand failure mode created under dynamic operating conditions. The use of such emerging and non-stabilized technologies imposes careful implementation of adequate Design Rules. In particular, dynamic stress (switch off and switch on inducing losses) for implementation of GaN Power Switch transistor devices is of particular concern and can be viewed in light of such generalized BAZ methodology proposed. As a consequence, design and reliability simulation tools are important threads to be under control. Design rules as well as electrical and physical characterizations are key phases to be structured.

9. Conclusion

The principle of the generalized BAZ model exposed in Ref. [2] was recalled. An example of a Normally-Off GaN Power switch transistor detailing from the data sheet the maximum rating limits was considered. We have seen how other dynamic maximum rating limits must be pondered in detail and in particular for switching bias operating conditions (also to be related to specific Design Rules to define).

The generalized BAZ model was refined and adapted to the GaN technology. As an example we have completed numerical Application on a Normally-off transistor GaN reference GS66508P-E03 650 V enhancement mode manufactured by GaN Systems. The concepts of maximum rating limits and burnout conditions have been useful to derive key parameters as χ_i's and γ's, both statistically represented by a normal distribution law. In particular such normalized stress factors χ_i vs the catastrophic burnout limit $S_{iBO\_failure}$ of a Normally-off transistor GaN were displayed. As a consequence, when multiple stresses are applied simultaneously, the derating parameters and their maximum rating limits values are imbricated to derive the equivalent effective activation energy.

To complete our approach, the BAZ Multiple Stress Model will be associated with the approach proposed by J. B. Bernstein related to the Multiple High-Temperature Operating Life (M-HTOL) test [11,12]. This extension will be developed in a future common paper under preparation.

Finally this model helps to assess the impact of the mission profile on the final activation energy expected and then assess margin to Design for Reliability Space equipments. This gives reliability quantification rule for effective E_a and related condition of stress to assess RUL (Remaining Useful Life) condition. We need to be very careful when applying Quality Standards which are not considering multiple-stressor impacts and new rules for HiRel application are recommended to be set accordingly. A short discussion was presented to recall the main advantages, drawbacks and some special care to implement the methodology.

Acknowledgments

The study was conducted in the frame of Electronic Robustness contract Robustness Project IRT-008 managed by IRT Saint Exupery, Toulouse (France) and sponsored by the following funding partners: Agence Nationale de la Recherche, Airbus Operations SAS, Airbus Group Innovation, Continental Automotive France, Thales Alenia Space France, Thales Avionics, Laboratoire d'Analyse et d'Architecture des Systèmes — Centre National de la Recherche Scientifique (LAAS-CNRS), Safran Labinal Power Systems, Bordeaux University, Institut National Polytechnique Bordeaux (IMS — UMR 5218), and Hirex engineering.

I would like to particularly thank Professor Ephraim Suhir for his expertise and valuable advices on the reliability topics, who has inspired me for the orientation of this paper. Thanks are going to my colleagues Bernardo Cougo and André Durier (Project Manager) at IRT Saint Exupery, for the fruitful discussions we had on e-GaN FET implementation and Power device modeling.

I would like to particularly thank Professor Joseph B. Bernstein, from Ariel University and Maryland University for the major comments and deep discussions we had during the final preparation of this manuscript and inspiring part of the conclusion of this paper.

References

[1] E. Wigner, The Transition State Method, 34Faraday Society (London) Trans, 1938 29–41.
[2] M. Evans, M. Polanyi, Inertia and Driving Force of Chemical Reaction, 34Faraday Society (London) Trans, 1938 11–29.
[3] E. Suhir, Predicted Reliability of Aerospace Electronics: Application of Two Advanced Probabilistic Concepts, IEEE Aerospace Conference, Big Sky, Montana, March 2-9, 2013 (Paper 2037).
[4] A. Bensoussan, E. Suhir, Design-for-reliability (DfR) of Aerospace Electronics: Attributes and Challenges, IEEE Aerospace Conference, Big Sky, Montana, Paper 2013, p. 2057 (March 2-9, 2013).
[5] J.W. McPherson, Reliability Physics and Engineering, Time-to-failure Modelling, second ed.Springer-Verlag, New York, NY, USA, 2013.
[6] B. Cougo, J. Brandelero, H. Schneider, T. Meynard, Accurate switching energy estimation of parallel eGaN FETs for modern aircraft applications, Proc. IEEE Wide Bandgap Power Devices Appl. 2013, pp. 108–111.
[7] B. Cougo, H. Schneider, T. Meynard, High current ripple for power density and efficiency improvement in wide bandgap transistor-based buck converters, IEEE Trans. Power Electron. 30 (8) (August 2015) 4489–4504.
[8] J. Brandelero, B. Cougo, T. Meynard, N. Videau, A Non-intrusive Method for Measuring Switching Losses of GaN Power Transistors, IECON, Vienna, Austria, 2013.
[9] J.A. Del Alamo, J. Joh, GaN HEMT reliability, Microelectron. Reliability 49 (9–11) (2009) 1200–1206, http://dx.doi.org/10.1016/j.microrel.2009.07.003.
[10] R.L. Agarwal, et al., Temperature dependence of the breakdown voltage for reverse-biased GaN p–n–n+ diodes, Solid State Commun. Volume 117 (Issue 9, 13) (February 2001) 549–553.
[11] J.B. Bernstein, M. Gabbay, O. Delly, Reliability Matrix Solution to Multiple Mechanism Prediction, Volume 54 (Issue 12) (December 2014) 2951–2955http://dx.doi.org/10.1016/j.microrel.2014.07.115.
[12] J.B. Bernstein, Reliability Prediction from Burn-in Data Fit to Reliability Models. Ariel University, Elsevier, ©2014http://dx.doi.org/10.1016/B978-0-12-800747-1.